



## Research Paper

## System reliability analysis of soil slopes with general slip surfaces using multivariate adaptive regression splines

Subhadeep Metya<sup>a,b,\*</sup>, Tanmoy Mukhopadhyay<sup>a</sup>, Sondipon Adhikari<sup>a</sup>, Gautam Bhattacharya<sup>b</sup><sup>a</sup> College of Engineering, Swansea University, Swansea, United Kingdom<sup>b</sup> Civil Engineering Department, Indian Institute of Engineering Science and Technology (IIST), Shibpur, India

## ARTICLE INFO

## Article history:

Received 27 September 2016

Received in revised form 18 January 2017

Accepted 21 February 2017

Available online 7 March 2017

## Keywords:

Slope stability

General slip surface

System reliability analysis

Multivariate adaptive regression splines

Monte Carlo simulation

Noise

## ABSTRACT

A data driven multivariate adaptive regression splines (MARS) based algorithm for system reliability analysis of earth slopes having random soil properties under the framework of limit equilibrium method of slices is considered. The theoretical formulation is developed based on Spencer method (valid for general slip surfaces) satisfying all conditions of static equilibrium coupled with a nonlinear programming technique of optimization. Simulated noise is used to take account of inevitable modeling inaccuracies and epistemic uncertainties. The proposed MARS based algorithm is capable of achieving high level of computational efficiency in the system reliability analysis without significantly compromising the accuracy of results.

© 2017 Elsevier Ltd. All rights reserved.

## 1. Introduction

It is now widely recognized that the soil parameters are uncertain, and thereby the conventional factor of safety based deterministic slope stability analyses are increasingly being replaced by slope reliability analyses under a probabilistic framework. In recent years, numerous slope reliability studies have been reported in the literature [1,2,3,4,6,5] assuming the single mode of failure, i.e., failure by sliding along a potential slip surface. There is also a growing appreciation that a slope can have many potential slip surfaces constituting a series system; and the probability of failure of the slope is greater than that associated with any one of these slip surfaces [7,8,9,10,11,12,13,14,15,16,17]. It has been commonly opined that the total or overall probability of failure of a slope (under the framework of system reliability) is the ultimate goal to achieve.

In the early studies [8,9,18], system failure probability of a slope is reported in terms of two bounds [19] which are sometimes widely separated. Most of the other studies fall under the two categories of methods suggested by Zhang et al. [13], namely, Method 1 and Method 2. In Method 1, the system failure probability is

evaluated directly by generating a large number of potential slip surfaces and performing Monte Carlo simulation (MCS) based on calculating the minimum factor of safety among them for each set of sampled values of soil properties (realisation) [12,20]. In Method 2, on the other hand, a few representative slip surfaces are first identified from amongst the large number of potential slip surfaces, and the system failure probability is then evaluated by performing Monte Carlo simulation based on calculating the minimum factor of safety among these representative slip surfaces for each realisation [21,16,22]. The results obtained from these two methods are found to be practically the same. Further, because the Monte-Carlo simulation requires high computational effort and time, several response surface methods (RSMs) have also been used for system reliability evaluations, e.g., polynomial-based RSM [23], Kriging methodology [24,25], the artificial neural network (ANN) [26], the support vector machine (SVM) [27], the high dimensional model representation (HDMR) [28], and others. An excellent review on the application of various RSMs for slope reliability analysis is available in the literature [29].

Alternatively, in order to evaluate the system reliability of a soil slope, for each set of sampled values of soil properties in a Monte Carlo analysis, one could find the critical slip surface and its corresponding minimum factor of safety [30,31] instead of finding the minimum factor of safety among a fixed set of slip surfaces generated before the simulation starts (as in Method 1 and Method 2). The overall probability of failure (or system failure probability),

\* Corresponding author at: College of Engineering, Swansea University, Swansea SA1 8EN, United Kingdom.

E-mail addresses: [884629@swansea.ac.uk](mailto:884629@swansea.ac.uk), [subhadeep.metya@gmail.com](mailto:subhadeep.metya@gmail.com) (S. Metya).

$p_{F, s}$ , will then be the ratio of the number of times the minimum factor of safety is less than 1.0 to the total number of simulation runs. While the former approach is more logical of the two approaches, the latter approach (as in Method 1 and Method 2) is computationally simpler and thus more commonly used in the literature. It is therefore necessary to investigate to what extent the results obtained based on the two approaches differ, as well as which approach leads to a more conservative estimate of the safety of a slope as a system. Further, whichever approach is used, it requires considerable computational effort and time. To enhance the computational efficiency, the relationship between the minimum factor of safety and the uncertain parameters is approximated by the multivariate adaptive regression splines (MARS) based surrogate model in this study. Although the application of MARS to geotechnical engineering field is not very common, only found recently in slope stability analysis by Liu and Cheng [32], its application in other fields of engineering is very much appreciated recently [33,34,35,36,37]. Moreover, previous studies have focused mainly on the application of various RSMs for approximating the relationship between the factor of safety and uncertain parameters. In this study, however, the MARS has been made use of not only to approximate the relationship between the minimum factor of safety and uncertain parameters, the location of the critical slip surfaces are also predicted by MARS. Thus the objective of the present study is also to explore the potential of MARS as an efficient mapping route in slope reliability analysis.

Furthermore, in almost all the previous studies on system reliability analysis of earth slopes, the shape of the slip surface is assumed as circular and the Bishop's simplified method (BSM) is used as a slope stability model. As the BSM does not satisfy horizontal force equilibrium, it is commonly regarded as an approximate method. The shape of actual slip surface is also, in general, not circular except in a homogeneous slope without discontinuities of any kind [38]. Keeping the above in view, in this study, while no assumptions have been made regarding the shape of the slip surface, the slope stability evaluation is based on the Spencer method valid for general slip surfaces [39] satisfying all conditions of static equilibrium, which is definitely more rigorous than the Bishop's simplified method, especially for non-homogeneous slopes.

## 2. Adopted methodologies

### 2.1. Slope stability analysis – deterministic and probabilistic

A typical slope, found in various civil engineering projects including dams, embankments and open cut for highways, is as shown in Fig. 1. The stability of these slopes along potential failure surfaces is of major interest. Slope stability analyses based on the limit equilibrium approach have conventionally been performed in a deterministic manner and the entire process consists of two

parts, namely, computation of factor of safety of a given or trial slip surface, and then search for the critical slip surface having the minimum factor of safety  $FS_{min}$  (known as the deterministic critical slip surface) using an optimization technique. The Spencer method of slices valid for general slip surfaces [39] is regarded as one of the rigorous methods as it does not make any a priori assumption regarding the shape of the slip surface and satisfies all conditions of equilibrium [40]. The computation of factor of safety (FS) in Spencer method involves solution of a pair of nonlinear stability equations. An efficient method of solution first formulates the problem as an optimization problem and then solves it using a powerful optimization technique [41]. Therefore, the deterministic slope stability analysis in this study leads to a 2-tier analysis and the optimization problem in each tier of analysis has been solved using the sequential quadratic programming (SQP) [42] technique which has been rated as a powerful optimization technique [31] and can be easily implemented in the MATLAB platform with its optimization toolbox.

Under the framework of single mode of failure, similar to the deterministic analysis, the probabilistic slope stability analysis can be viewed as the problem of locating the slip surface corresponding to the lowest value of reliability index  $\beta_{min}$  (or the highest value of the probability of failure), called the probabilistic critical slip surface of the slope. The first order reliability method, (FORM) which is widely accepted as the most versatile among the approximate methods of reliability analysis [43], has been adopted in this study. The computational procedure for the determination of the probabilistic critical slip surface based on FORM involves a 3-tier optimization: (i) evaluation of performance function requiring the evaluation of Spencer's factor of safety involves the first tier of optimization; (ii) evaluation of the reliability index,  $\beta$  based on FORM involves the second tier of optimization, and (iii) the search for the surface of minimum reliability index ( $\beta_{min}$ ) involves the third tier of optimization. The SQP technique has been employed in the MATLAB platform to solve the optimization problem involved in each tier of analysis. More detailed description of the computational procedure for the determination of the probabilistic critical slip surface based on FORM can be found elsewhere [4,44,45]. The computer program developed and used in the referred studies was validated with reference to two benchmark slope problems. The availability of such a computer program has been made use of in the present study for the purpose of determination of the probabilistic critical slip surface.

### 2.2. MARS-based MCS for system reliability analysis of slopes

#### 2.2.1. Formulation of Multivariate Adaptive Regression Splines (MARS)

An efficient mathematical relationship between input parameters and output feature of interest for a system under investigation based on few algorithmically chosen samples can be established with the help of MARS [33]. It is a nonparametric regression proce-

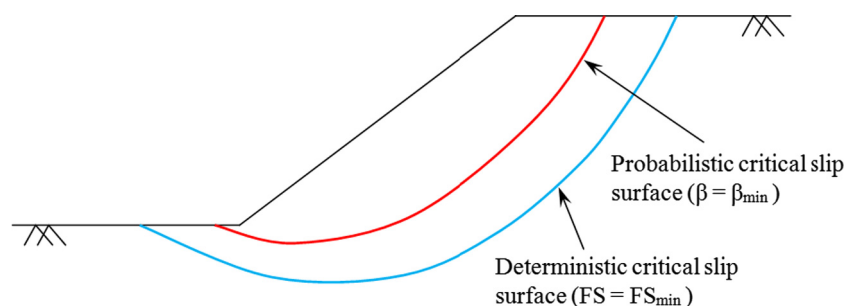


Fig. 1. A typical slope with potential slip surfaces.

ture that makes no supposition about the underlying functional connection between the dependent and independent variables. MARS algorithm adaptively selects a set of ‘basis functions’ for approximating the response function through a forward and backward iterative approach. The MARS model can be expressed as

$$Y = \sum_{k=1}^n \alpha_k H_k^f(x_i) \tag{1}$$

with  $H_k^f(x_1, x_2, x_3, \dots, x_n) = 1$ , for  $k = 1$

where  $\alpha_k$  and  $H_k^f(x_i)$  are the coefficient of the expansion and the ‘basis functions’ respectively. Thus the first term in Eq. (1) becomes  $\alpha_1$ , which is basically an intercept parameter. The ‘basis function’ can be represented as

$$H_k^f(x_i) = \prod_{j=1}^{i_k} [Z_{i,k}(x_{j(i,k)} - t_{i,k})]^q \tag{2}$$

where  $i_k$  is the number of factors (interaction order) in the  $k$ -th basis function,  $Z_{i,k} = \pm 1$ ,  $x_{j(i,k)}$  is the  $j$ -th variable,  $1 \leq j(i,k) \leq n$ , and  $t_{i,k}$  is a knot location on each of the corresponding variables.  $q$  is the order of splines. The approximation function  $Y$  is composed of ‘basis functions’ associated with  $k$  sub-regions. Each multivariate spline ‘basis function’  $H_k^f(x_i)$  is the product of univariate spline basis functions  $z_{i,k}$ , which is either order one or cubic, depending on the degree of interrelationship of the approximation. The notation “ $tr$ ” means the function is a truncated power function.

$$[Z_{i,k}(x_{j(i,k)} - t_{i,k})]_{tr}^q = [Z_{i,k}(x_{j(i,k)} - t_{i,k})]^q \text{ for } ; [Z_{i,k}(x_{j(i,k)} - t_{i,k})] < 0 \tag{3}$$

$$[Z_{i,k}(x_{j(i,k)} - t_{i,k})]_{tr}^q = 0, \text{ otherwise} \tag{4}$$

Here each function is considered as piecewise linear with a trained knot ‘ $tr$ ’ at each  $x_{i,k}$ . Now allowing the basis function to bend at the knots, MARS can model functions that differ in behaviour over the domain of each variable. This is applied to interaction terms as well. The interactions are no longer treated as global across the entire range of predictors but between the sub-regions of every ‘basis function’ generated. Depending on fitment, the maximum number of knots to be considered, the minimum number of observations between knots, and the highest order of interaction terms are calculated. The screening of automated variables occurs as a result of using a modification of the generalized cross-validation (GCV) model fit criterion, developed by Craven and Wahba [46]. MARS identifies the location and number of the needed spline ‘basis functions’ in a forward or backward stepwise fashion. It starts by overfitting a spline function through each knot, and then by removing the knots that least contribute to the overall fit of the model as determined by the modified GCV criterion, often completely eliminating the most insignificant variables. Eq. (5) depicts the lack-of-fit ( $L_f$ ) criterion used by MARS.

$$L_f(Y_{\tilde{k}}) = G_{cv}(\tilde{k}) = \frac{\frac{1}{n} \sum_{i=1}^n [Y_i - Y_{\tilde{k}}(x_i)]^2}{\left[1 - \frac{\tilde{c}(\tilde{k})}{n}\right]^2} \tag{5}$$

where  $\tilde{c}(\tilde{k}) = c(\tilde{k}) + M\tilde{k}$ .

where ‘ $n$ ’ denotes the number of sample observations,  $\tilde{c}(\tilde{k})$  is the number of linearly independent ‘basis functions’,  $\tilde{k}$  is the number of knots selected in the forward process, and ‘ $M$ ’ is a cost for basis-function optimization as well as a smoothing parameter for the procedure. Larger values of ‘ $M$ ’ result in fewer knots and smoother function estimates. The best MARS approximation is the one having the highest GCV value. Thus MARS is also compared with parametric and nonparametric approximation routines in terms of its accuracy, efficiency, robustness, model transparency,

and simplicity and it is found suitable methodologies because it is more interpretable than most recursive partitioning, neural and adaptive strategies wherein it distinguishes well between actual and noise variables. Moreover, the MARS models are reported [47] to work satisfactorily in terms of computational cost irrespective of dimension (low-medium-high) and noise.

### 2.2.2. Proposed procedure for system reliability analysis using MARS-based MCS

As already mentioned, an earth slope with uncertain soil parameters is often characterized by the presence of numerous potential slip surfaces and more importantly these are not known beforehand and are determined as part of the analysis. Let  $N_s$  be the number of potential slip surfaces identified in a slope, and  $S_i$  denote the  $i$ th one,  $i = 1, 2, \dots, N_s$ . In this study to evaluate the system probability of failure, the slope has been viewed as a series system in which each potential slip surface is a component and the critical slip surface is the weakest one. A slope as a series system fails when an event of failure occurs along any of these slip surfaces. The minimum factor of safety ( $FS_{min}$ ) determined under an uncertain environment is used as a performance indicator of the slope. In Monte Carlo simulation, if the performance function of the  $j$ th sample is given by  $g(\mathbf{X}^j)$ , then a safety judgement for each trial can be provided as follows:

$$\delta(\mathbf{X}^j) = \begin{cases} 1, & \text{if } g(\mathbf{X}^j) = FS_{min} - 1 \leq 0 \\ 0, & \text{if } g(\mathbf{X}^j) = FS_{min} - 1 > 0 \end{cases} \tag{6}$$

Then, an estimate of the system failure probability can be obtained by

$$p_{F,s} = \frac{1}{N} \sum_{j=1}^N \delta(\mathbf{X}^j) \tag{7}$$

where  $N$  is the total number of simulation cycles. An important point to be noted here is that in this proposed procedure the optimum number of simulations required intuitively indicates the number of potential slip surfaces to be analyzed (i.e.,  $N_s = N$ ) for an accurate system reliability analysis. As the value of probability of failure obtained from MCS is known to be sensitive to the number of simulations, to assess the accuracy and the efficiency of the proposed procedure, the optimum number of simulations is first identified and the COV of the  $p_{F,s}$  is then estimated [using Eq. (8)] to compare the results obtained from other methodologies.

$$COV_{p_f} = \sqrt{\frac{(1 - p_{F,s})}{N \times p_{F,s}}} \tag{8}$$

As already indicated, using the above procedure based on any deterministic slope stability model (LEM or FEM), the computational cost involved is very high. In this study, therefore, an efficient surrogate model is used to map the minimum factor of safety as well as the location of the corresponding critical slip surface as function of the uncertain soil parameters. The entire procedure is executed in two stages. In stage 1, an explicit form of MARS based surrogate model is constructed to map the implicit relationship between the  $FS_{min}$  and the uncertain shear strength parameters. Then in stage 2, the scheme of MCS explained above is conducted using MARS based surrogate, in place of the actual deterministic slope stability model, by locating deterministic critical slip surface and the corresponding  $FS_{min}$ . In comparison to the direct MCS, the computational time needed for this procedure is significantly reduced as only a few numbers of run of the original deterministic stability analysis are required to set up the MARS based surrogate.

A flowchart to summarize the proposed procedure for the system reliability analysis of a soil slope based on the MARS-based

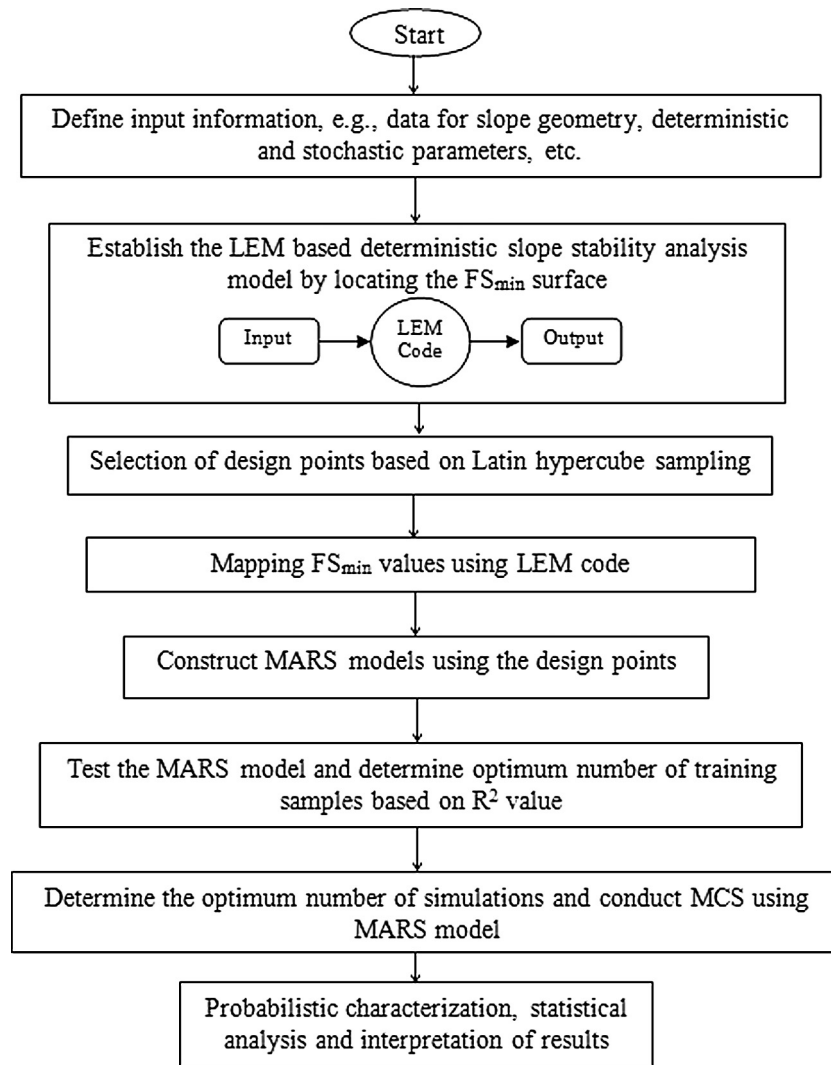


Fig. 2. Flowchart of stochastic analysis using MARS model.

MCS is shown in Fig. 2. The detailed procedure has the following steps.

**Step 1:** Define input information: Define the necessary input parameters needed to describe the slope geometry and soil layer boundaries, the parameters which are of deterministic nature and the stochastic parameters with their statistical properties (i.e., mean and COV).

**Step 2:** Establish the deterministic stability analysis model for locating the deterministic critical slip surface and the associated minimum factor of safety (as presented in the first paragraph of Section 2.1). Here the commonly used curvature constraint on kinematical admissibility (upward concavity of the shape of a slip surface) is imposed.

**Step 3:** Generate training samples by Latin hypercube sampling (LHS) and calculate the  $FS_{min}$  values as well as the co-ordinates of the corresponding critical slip surface location for each data set using the LEM based code developed in Step 2.

In slope stability computations, it is widely known that the accuracy of calculation of the values of  $FS_{min}$  (as well as the co-ordinates of the discrete points on the corresponding critical slip surface of general shape) is influenced by the slice division in the potential slip surface. This influence is generally substantial up to

a certain number of slices beyond which this influence becomes small or insignificant for all practical purposes. In this context it may be mentioned that the proposed methodology does not put any restriction on the number of slices. However, it is conceivable that greater the number of slices, greater will be the computing time and, consequently, lower will be the efficiency of the method. Keeping this in view, in a given slope problem, based on a sensitivity study carried out by increasing the number of slices, an optimum number of slices can be found out beyond which there is no significant improvement (decrease) in the value of  $FS_{min}$ .

**Step 4:** Construct the MARS based surrogates to map the minimum factor of safety as well as to predict the location of the critical slip surface.

**Step 5:** Test the output of the MARS based response surface and determine the optimum numbers of training samples based on the value of the coefficient of determination ( $R^2$ ).

**Step 6:** To evaluate the system failure probability  $p_{F,S}$ , run the trial MCS, predict the  $FS_{min}$  surface and the  $FS_{min}$  value using the MARS models developed (in steps 4 and 5) for each sample run and determine the optimum number of simulation ( $N$ ). As discussed before, this gives the total number of failure modes or potential slip surfaces to be analyzed,  $N_s = N$ .

Apparently, in step 6, for prediction of the critical slip surface locations ( $FS_{\min}$  surfaces) there is no need for imposing the curvature constraints mentioned in step 2. However, the MARS model, being a response surface equation (RSM), cannot be expected to make 100% accurate predictions. Thus, it is quite likely that a few predicted slip surfaces remain kinematically inadmissible.

Therefore, it is required also to check whether all the predicted critical slip surface locations are acceptable or not by imposing that constraint. If, for a certain sample, the predicted surface is unacceptable, then that sample should be discarded from the run and the next sample is to be tried.

**Step 7:** Calculate the system failure probability,  $p_{F,s}$  and the COV associated with it ( $COV_{p_{F,s}}$ ). A COV value of more than 10% is generally considered as unacceptable.

In this context, it is useful to mention the guidelines for determining the sample size, as given below.

(i) Guideline for determining the sample size in establishing the MARS model:

In establishing the MARS model, one commonly used guideline for determining the sample size is that the value of the coefficient of determination ( $R^2$ ) should be greater than a pre-assigned quantity (0.95). It may be mentioned that Liu and Cheng [32] have also used this guideline. However, a more direct guideline is to make a plot of  $R^2$  versus number of samples and pick that value of abscissa as the sample size at which the fluctuation in the ordinate has become negligibly small. In this study the latter guideline has been made use of.

(ii) Guideline for determining the sample size in evaluating the system probability of failure:

In evaluation of system probability of failure, one commonly used guideline for determining the sample size is that the coefficient of variation (COV) of the probability of failure ( $p_{F,s}$ ) should be less than a pre-assigned quantity (0.15). It may be mentioned that Liu and Cheng [32] have also used this guideline. However, a more direct guideline is to make a plot of  $p_{F,s}$  versus number of samples and pick that value of abscissa as the sample size at which the fluctuation in the ordinate has become negligibly small. In this study the latter guideline has been made use of.

### 2.3. Effect of simulated noise on MARS based uncertainty quantification scheme

Amongst the various sources of parameter uncertainty [Fig. 3a], random testing error or noise is one of the important sources in many problems. Random testing errors arise from factors related

to the measuring process such as operator error or a faulty device, test imperfections, soil specimen disturbance, limited size of specimens, differences between in-situ and laboratory stress conditions, use of imperfect empirical correlations, error in modeling and computer simulation. These are also termed as epistemic uncertainties by some authors [48,49]. Therefore, one should first identify the presence of any random testing error or noise and try to eliminate it. However, it is very difficult to fully eliminate these sources. Therefore, the performance of any modern uncertainty propagation algorithm should be studied with the influence of noisy datasets.

An analysis to explore the effect of simulated noise on MARS based uncertainty quantification scheme for soil slopes is taken up in this section. Gaussian white noise with a specific variance level ( $p$ ) is introduced in the set of output responses (the minimum factor of safety) [51] which is subsequently used for MARS model formation, as in Eq. (9).

$$F_{iM} = f_i + p \times \xi_i \quad (9)$$

where  $f$  denotes the minimum factor of safety and the subscript  $i$  is the sample number in the design point set.  $\xi_{ij}$  is a function that generates normally distributed random numbers. Subscript  $M$  is used here to indicate the minimum factor of safety including the effect of noise.

Subsequently, the simulated noisy dataset (i.e. the sampling matrix for MARS model formation) is created by introducing pseudo random noise in the responses, while the input design points are kept unchanged. Then for each dataset, MARS based MCS is carried out to quantify uncertainty of soil slopes, as described in Fig. 3b. Effect of noise are found to be accounted for in several other studies in the available literature [52,53] dealing with deterministic analysis. Assessment of any surrogate based uncertainty propagation algorithm under the effect of noise in the field of geotechnical engineering is the first attempt of its kind to the best of the authors' knowledge. It is necessary to take into account such simulated noise considering the presence of other sources of uncertainty such as error in measurement of responses, error in modeling and computer simulation and various other epistemic uncertainties involved with the system. Thus the kind of analysis carried out here will provide a comprehensive idea about the robustness of the MARS based model under noisy data.

### 3. Illustrative examples and results

To elucidate the methodology presented in the preceding section, two example problems are selected from the literature. Example 1 concerns a simple slope in a 2-layered soil with horizontal layer boundary and Example 2, a complex slope in a multilayer ( $c, \phi$ ) soil with arbitrary layer boundaries.

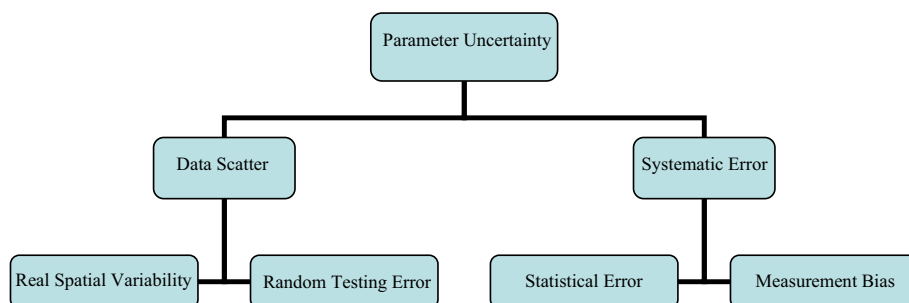


Fig. 3a. Sources of parameter uncertainty (after [50]).

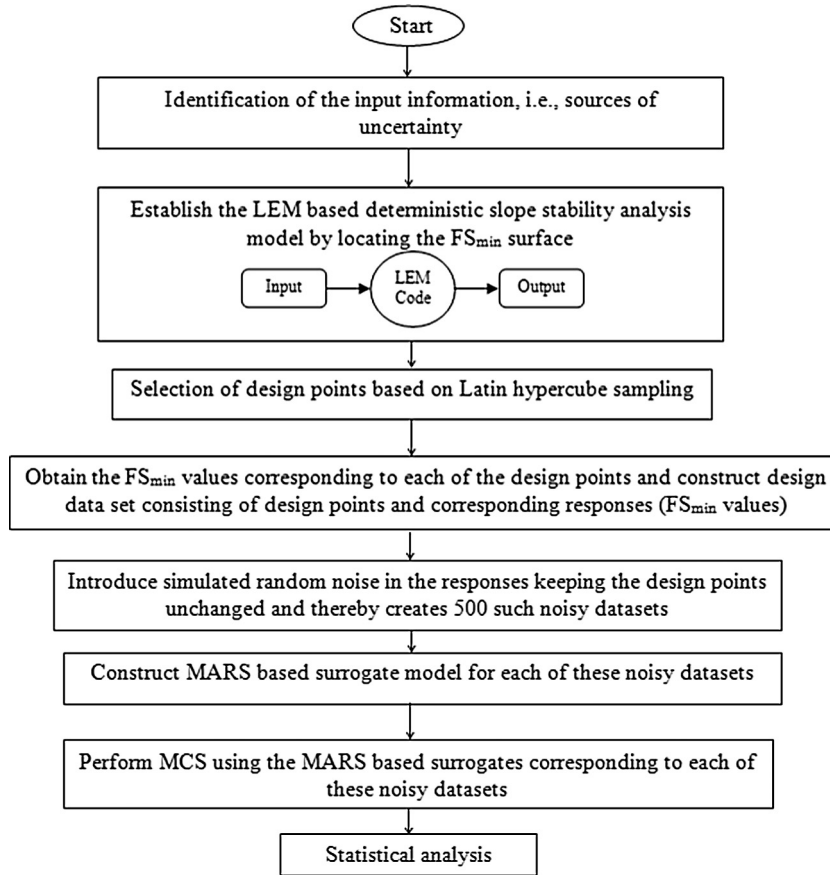


Fig. 3b. Flowchart for analyzing the effect of noise on the MARS based uncertainty quantification algorithm.

3.1. Example 1

A simple slope in a two-layer soil: An embankment underlain by soft clay foundation [54]

Fig. 4 shows an embankment underlain by a soft clay foundation, taken from Ji et al. [54]. The undrained shear strength of the soft clay  $c_2$  is considered as a normally distributed random variable with a mean value of 25 kN/m<sup>2</sup> and a coefficient of variation of 0.25. All the other strength parameters of the two layers are assumed to be deterministic with values as given in Fig. 4. It may be pointed out that previously Ji et al. [54] analyzed this problem assuming slip surfaces to be of circular shape. In the present study, as mentioned before, there is no a priori assumption regarding the geometry of the slip surface. In other words, slip surfaces of general shape have been considered. Further, based on the discussion in

step 3 under Section 2.2.2, the number of slice division is selected as 12.

Initially, taking the value of cohesion of the soft clay foundation as 25 kPa (equal to its mean value), the deterministic critical slip surface of general shape has been located (Fig. 5) and the corresponding minimum factor of safety ( $FS_{min}$ ) is obtained as 1.311 using the Spencer method [39] coupled with the SQP method of optimization. A  $FS_{min}$  value of 1.462 was reported by Ji et al. [54] using the Spencer method with a circular slip surface. It is therefore observed that the value of the minimum factor of safety ( $FS_{min}$ ) as obtained in the present analysis is lower (nearly 10%) than that reported by Ji et al. [54].

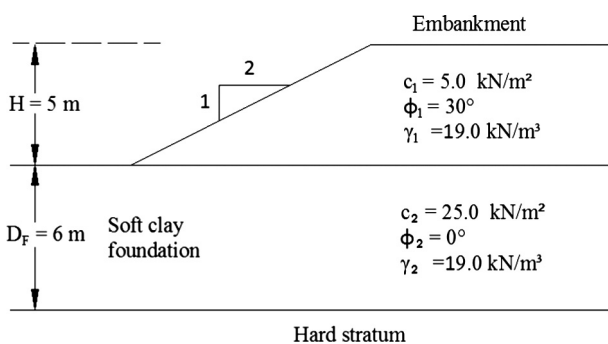


Fig. 4. Slope section in example 1 [54].

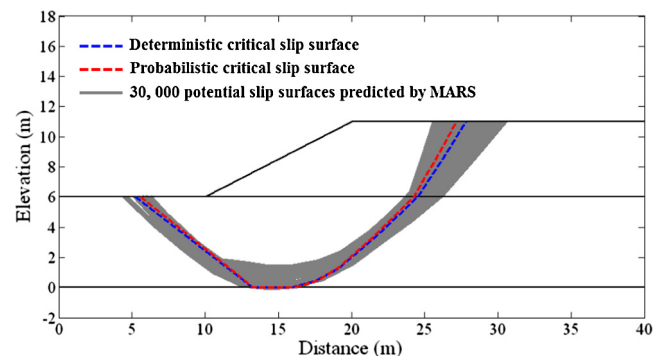


Fig. 5. Slope section and the different critical slip surface locations (namely, the deterministic critical slip surface, the probabilistic critical slip surface and the 30,000 potential slip surfaces predicted by MARS) in example 1.

Next, considering the single mode of failure, the probabilistic critical slip surface has been determined based on the FORM and the associated minimum reliability index is obtained as  $\beta_{min} = 1.006$  [the corresponding value of  $p_F = \Phi(-\beta_{min})$  is obtained as  $1.57 \times 10^{-1}$ ]. It may be noted that the value of  $\beta_{min}$  obtained in the present study is significantly lower (nearly 24%) than that reported by Ji et al. [54] (i.e., 1.32) using circular slip surface. Fig. 5 presents the location of the probabilistic critical slip surface alongside the deterministic critical slip surface, which shows that these two critical slip surfaces are significantly different.

In order to study the system reliability analysis of this slope example, at first, some training samples are generated by Latin hypercube sampling (LHS) and the MARS based surrogate model is then constructed using these training samples to approximate the minimum factor of safety functional. To test the MARS model, the obtained  $FS_{min}$  values are compared for another 100 samples and the value of the coefficients of determination ( $R^2$ ) is determined. The optimum number of training samples is determined as 128 by varying the sample size from 16 to 1024 (powers of 2) (Fig. 6) and the corresponding value of  $R^2$  equals to 0.994. Fig. 7 presents the comparison between the values of  $FS_{min}$  predicted by different MARS models and those calculated by the Spencer method coupled with the SQP method, which indicates very good fitting and predictive capability of the MARS with 128 samples. The probability density function plots of the minimum factor of safety as presented in Fig. 8 also shows a negligible deviation between MARS model and original LEM model based on Spencer method indicating validity and high level of precision for the present surrogate based approach further.

Then, following the same procedure, MARS models are also constructed to predict the locations of the critical slip surface with numbers of slices equals to 12. For 10 arbitrary set of samples, predicted locations of critical slip surfaces are compared with the calculated locations using the Spencer method coupled with the SQP method in Fig. 9, which again indicates very good predictive capability of the MARS model.

The COV of the minimum factor of safety due the randomness added to slope system due to the presence of  $c_2$  as random is obtained as 22.1% using the MARS based surrogate. Another study based on the MARS based surrogate model to show the variation of the minimum factor of safety with variation of the random strength parameters in a normalised scale is depicted in Fig. 10, which shows that the nature of this variation is best fitted by a polynomial of order 3.

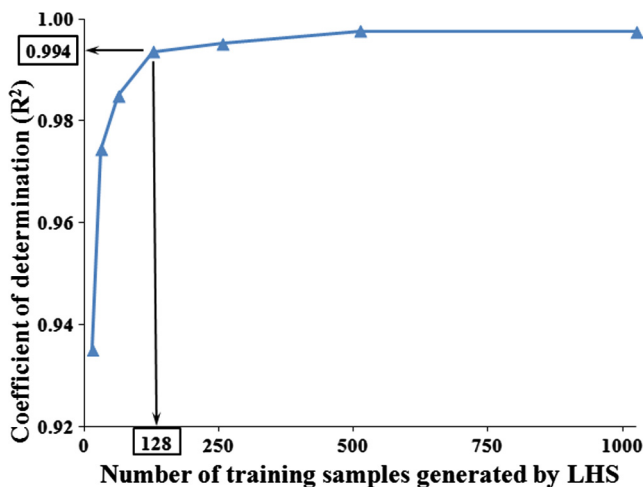


Fig. 6. Relationship between sample size and coefficient of determination ( $R^2$ ) (example 1).

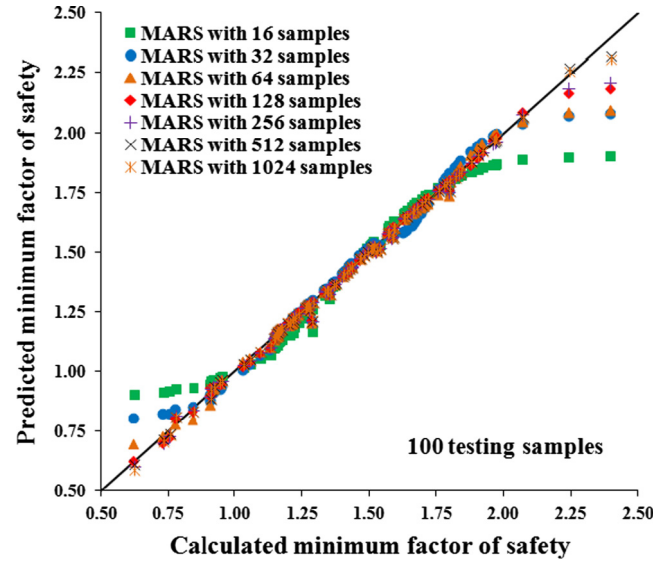


Fig. 7. Comparison between the values of  $FS_{min}$  predicted by different MARS models and those calculated by the Spencer method coupled with the SQP method in example 1.

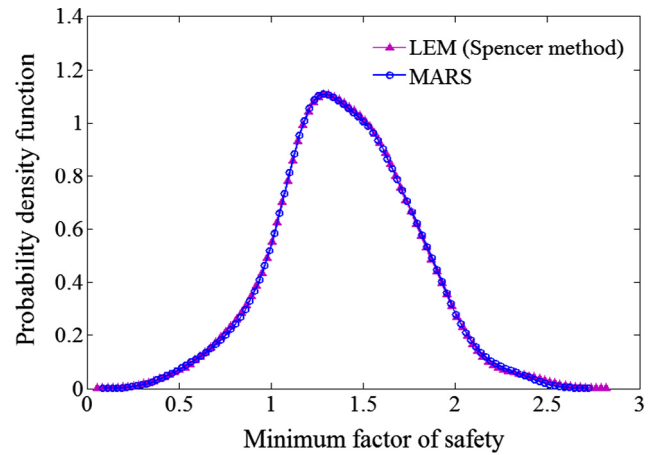


Fig. 8. Probability density function for minimum factor of safety based on the LEM (Spencer method) as well as those based on the constructed MARS model in example 1.

As the value of probability of failure obtained from MCS is known to be sensitive to the number of simulations, trial simulations have been conducted using the constructed MARS-based RSM by varying the sample size from 2500 to 50,000. Fig. 11 shows the sensitivity of the probability of failure to the sample size when the seed number is taken as 28061987 (an arbitrary value). It is seen that beyond a sample size of 30,000 the probability of failure  $p_F$  is not sensitive to the sample size, and hence, the same has been adopted as the optimum number of simulations. The corresponding value of system failure probability is obtained as  $1.73 \times 10^{-1}$ . In Fig. 5, the 30,000 potential slip surfaces predicted by MARS are plotted corresponding to the system failure probability determined above. Figs. 12a and 12b present the histograms with the corresponding normal fit for the abscissas and ordinates of vertices 1, 4, 7, 10 and 13 respectively.

Table 1 presents a comparison of the failure probabilities obtained in the present analysis and that reported by Ji et al. [54]. It is observed that the value of the system failure probability ( $p_{F,s}$ ) obtained in the present analysis is higher than those reported

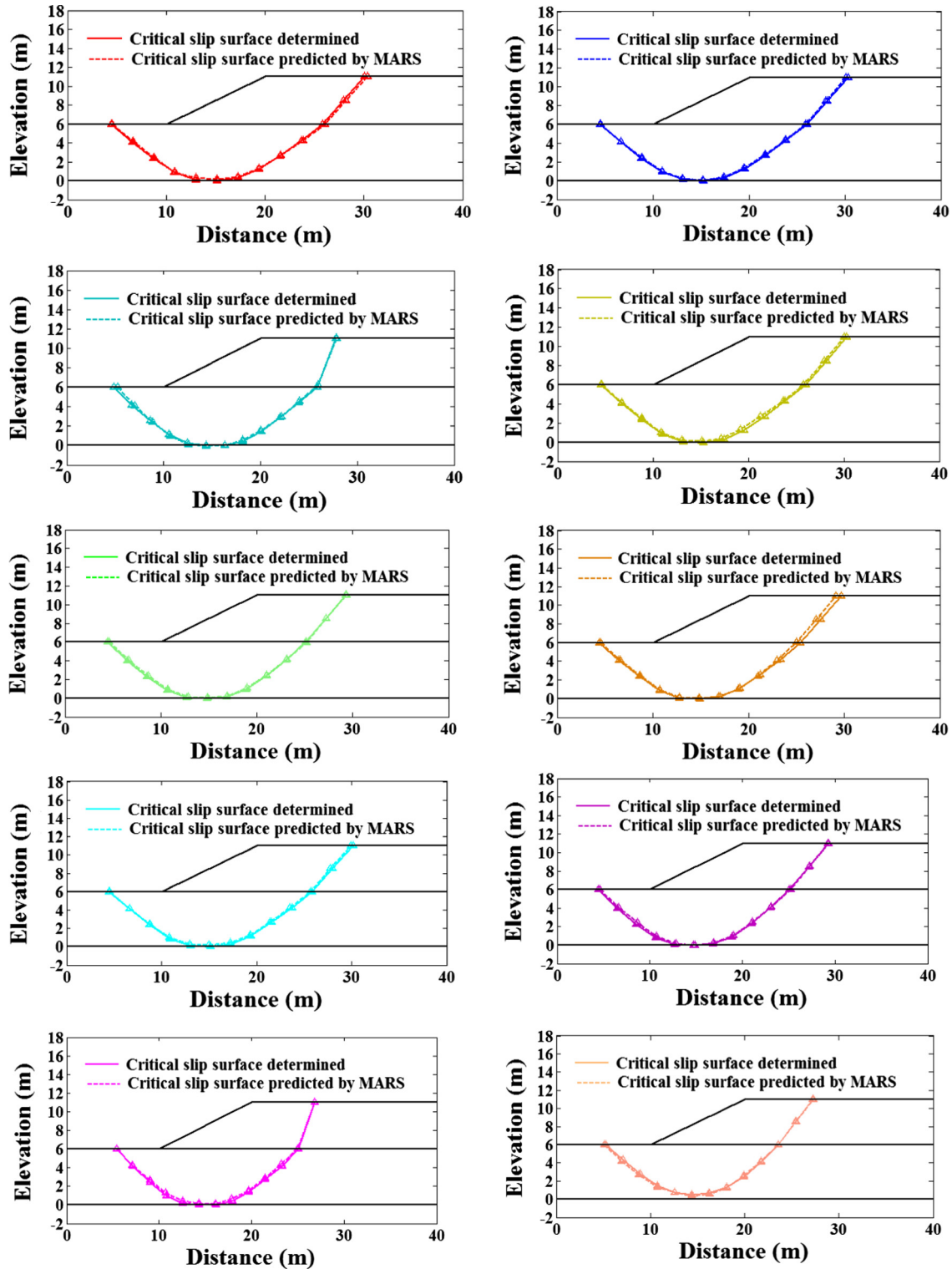


Fig. 9. Comparison between the locations of the critical slip surfaces determined by the Spencer method coupled with the SQP method and those predicted by MARS for 10 arbitrary set of samples in example 1.

in Ji et al. [54] using circular slip surfaces. It is also noted that system failure probability value is higher than the value of probability of failure associated with the probabilistic critical slip surface in the present study (assuming single mode of failure), which is as per expectation. It may be noted that the obtained system failure probability value of 17.3% indicates the performance level of the slope as ‘hazardous’ according to the [55].

### 3.2. Effect of noise

Representative results presented in Fig. 13 show the effect of noise on the minimum factor of safety. Gaussian white noise with a specific value of variance ( $p$ ) in the range of 0.01–0.5 is introduced in the set of minimum factor of safety, which is used for MARS model formation. The results furnished in this article are



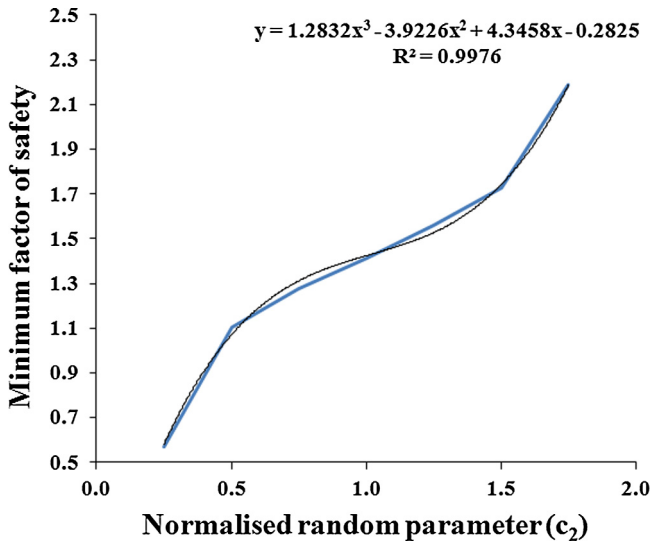


Fig. 10. Variation of the  $FS_{min}$  with  $c_2$  in example 1.

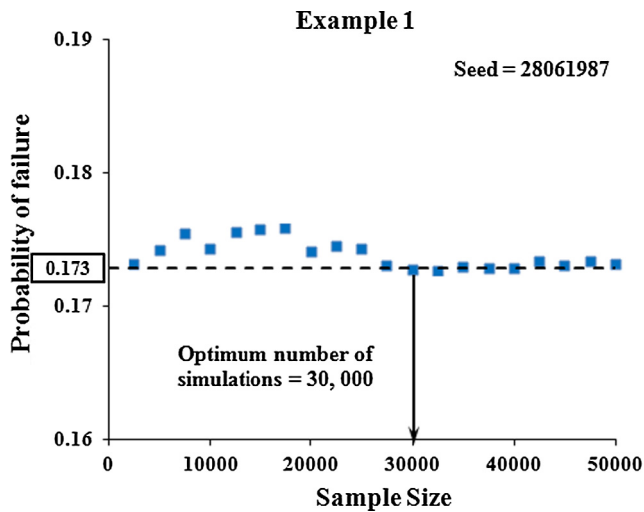


Fig. 11. Relationship between sample size and probability of failure (example 1).

obtained by using 500 such noisy datasets, which comprises the formation of MARS model and thereby carrying out MCS for each dataset using corresponding surrogate models [refer Fig. 3b]. The results presented for different values of variance are compared with the probability density function of noise-free case to provide a comprehensive idea about the performance of MARS in uncertainty quantification under the influence of simulated noise for minimum factor of safety of earth slopes.

### 3.3. Example 2

A complex slope in a multilayer ( $c, \phi$ ) soil with arbitrary layer boundaries (ACADS Study [56]).

This example is taken from the ACADS study [56] and is also considered by Ji and Low [14], Zhang et al. [16], Kang et al. [57] and Liu and Cheng [32] in their analysis. Fig. 14 shows the geometry of the multilayered slope that consists of three layers of different materials, and the layer boundaries are not entirely horizontal. Table 2 presents soil parameters for this slope. Strength parameters of layer 2 and layer 3 are considered as random variables and all these variables are assumed to be normally distributed. In the present study, as mentioned in example 1, slip surfaces of general shape have been considered, and, further, based on the discussion in step 3 under Section 2.2.2, the number of slice division is selected as 12.

Initially, like the example 1, assuming the soil properties to be deterministic with values equal to their mean values (Table 2), the deterministic critical slip surface of general shape has been located and is as shown in Fig. 15. The associated minimum factor of safety based on the Spencer method [39] is obtained as  $FS_{min} = 1.35$ . The recommended solution by the experts in the ACADS study is 1.39. Table 3 presents a comparison of the values of  $FS_{min}$  obtained in the present analysis and that reported by previous investigators. It is observed that the value of the minimum factor of safety ( $FS_{min}$ ) obtained in the present analysis is lower (nearly 4%) than those reported in the previous studies.

Like example 1, assuming the single mode of failure, the probabilistic critical slip surface has been determined based on the FORM and the associated minimum reliability index is obtained as  $\beta_{min} = 2.24$  [the corresponding value of  $p_F = \Phi(-\beta_{min})$  is obtained as  $1.25 \times 10^{-2}$ ]. Fig. 15 presents the location of the probabilistic critical slip surface alongside the deterministic critical slip surface,

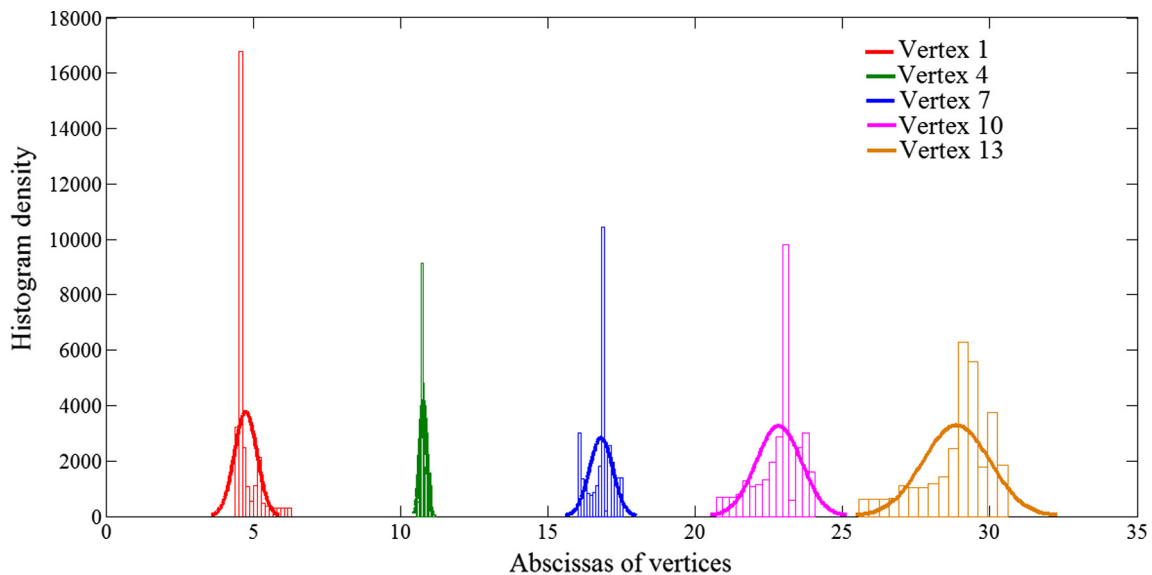


Fig. 12a. Histogram density plot of the abscissas of vertices in example 1.

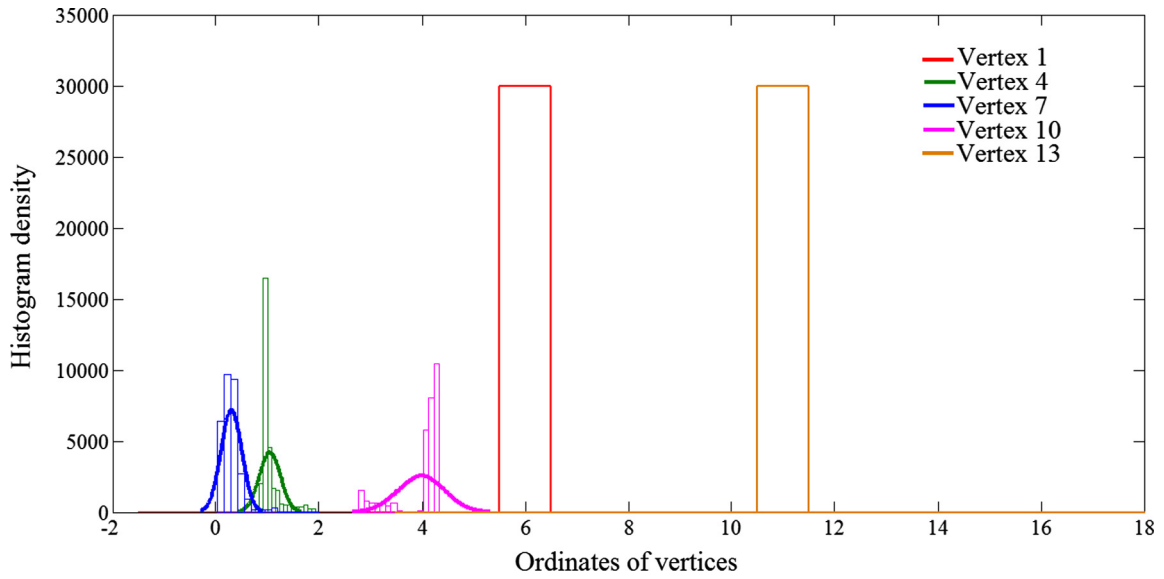


Fig. 12b. Histogram density plot of the ordinates of vertices in example 1.

Table 1

Summary of results of probabilistic analyses for example 1.

Studies	Probabilistic method	Probability of failure, $p_F$ (%)
Ji et al. [54]	Failure probability of the most critical slip surface based on the FORM (circular slip surface)	9.34% ( $\beta_{min} = 1.32$ )
Present study	Failure probability of the most critical slip surface based on the FORM (slip surface of general shape)	15.7% ( $\beta_{min} = 1.006$ )
	System failure probability based on MCS using the MARS based RSM (30,000 samples)	17.3% (COV = 1.71%)

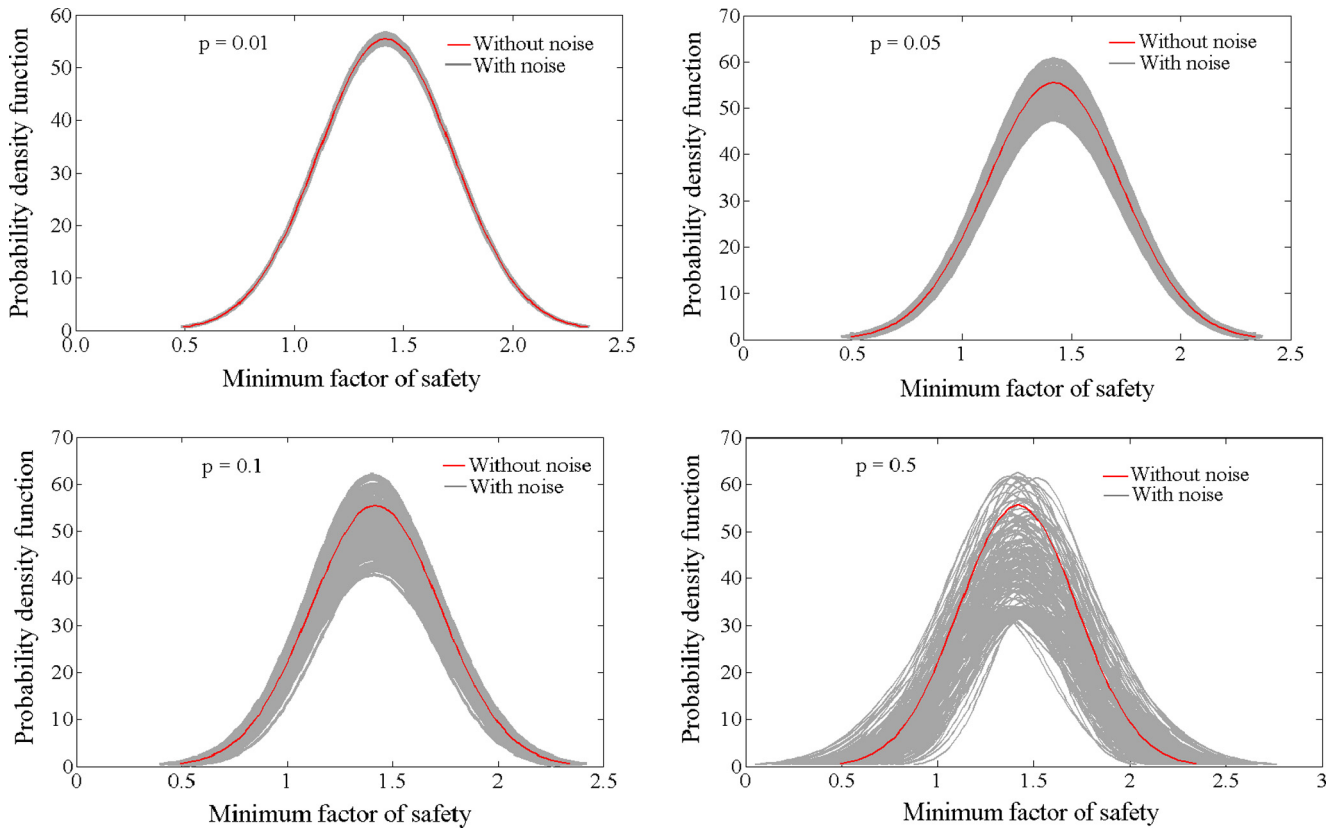


Fig. 13. Effect of noise on MARS based uncertainty quantification for minimum factor of safety of example 1.

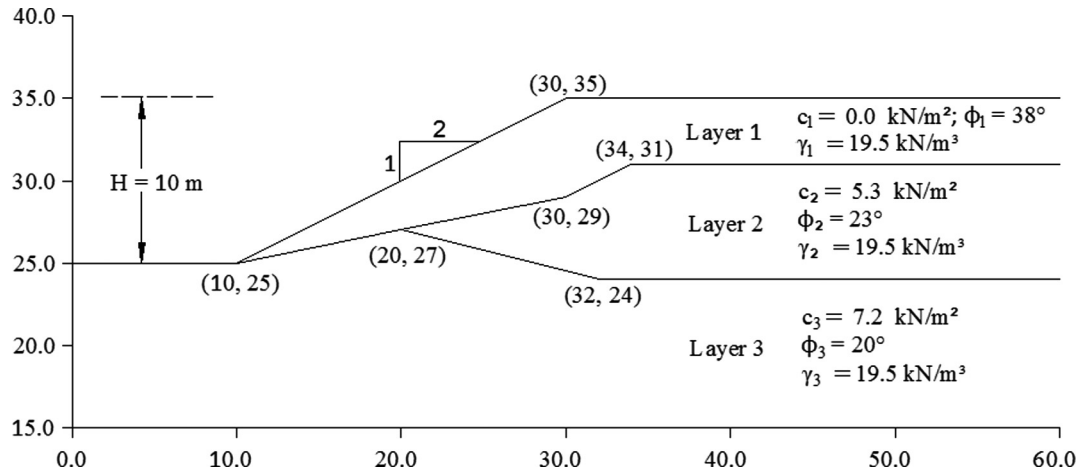


Fig. 14. Slope section in example 2.

Table 2  
Statistical properties of soil parameters for example 2.

Layers	Cohesion, $c$ (kN/m <sup>2</sup> )		Friction angle, $\phi$ (°)		Unit weight, $\gamma$ (kN/m <sup>3</sup> )
	Mean	COV (%)	Mean	COV (%)	
1	0.0	–	38.0	–	19.5
2	5.3	30	23.0	20	19.5
3	7.2	30	20.0	20	19.5

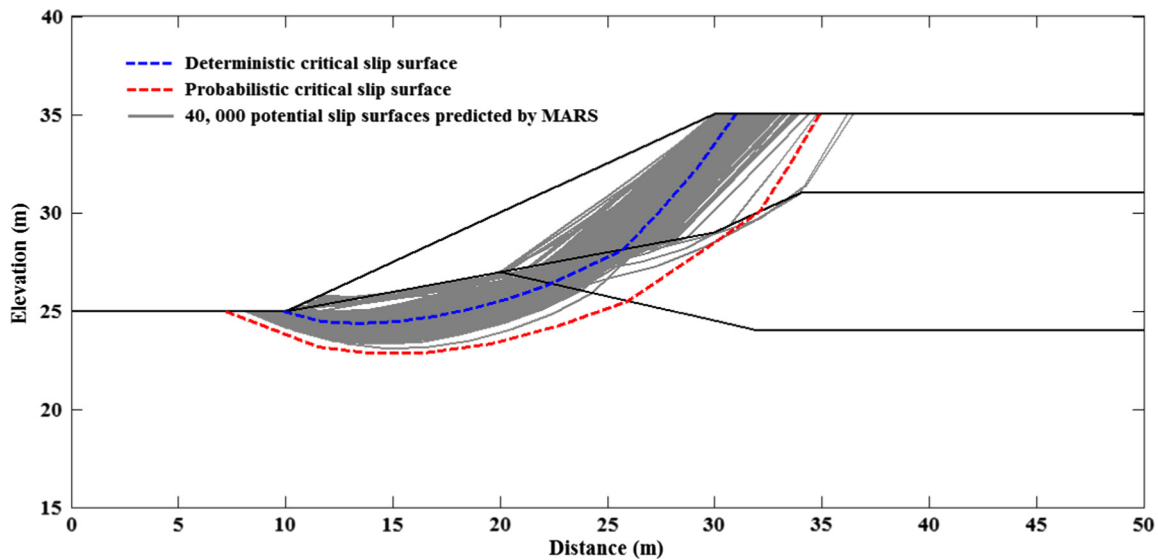


Fig. 15. Slope section and the different critical slip surface locations (namely, the deterministic critical slip surface, the probabilistic critical slip surface and the 40,000 potential slip surfaces predicted by MARS) in example 2.

which shows that these two critical slip surfaces are markedly different in shape and location.

As has been done for the example 1, for the system reliability analysis, at first, some training samples are generated by Latin hypercube sampling (LHS) and the MARS based surrogate model is then constructed using these training samples to approximate the minimum factor of safety functional. To verify the MARS model, the obtained  $FS_{min}$  values are compared for another 100 samples and the value of the coefficient of determination ( $R^2$ ) is determined. The optimum number of training samples is determined as 512 by varying the sample size from 16 to 1024 (pow-

ers of 2) (Fig. 16) and the corresponding value of  $R^2$  equals to 0.99. Fig. 17 presents a comparison between the values of  $FS_{min}$  predicted by different MARS models and those calculated by the Spencer method coupled with the SQP method of optimization, which indicates very good fitting and predictive capability of the MARS with 512 samples. Like example 1, the probability density function plots of the minimum factor of safety as presented in Fig. 18 also shows a negligible deviation between MARS model and original LEM model based on Spencer method indicating validity and high level of precision for the present surrogate based approach further.

**Table 3**  
Summary of results of deterministic analyses for example 2.

Studies	Slip surface shape	Methodology used			Minimum Factor of safety $FS_{min}$
		Limit equilibrium method	Method of solving the factor of safety equations for a specific slip surface	Optimization technique to search for the critical slip surface	
Ji and Low [14]	Circular	Spencer (1967)	Not available	Not available	1.406
Zhang et al. [16]	Circular	Bishop (1955)	Not required	Not available	–
Kang et al. [57]	Circular	Bishop (1955)	Not required	Not available	1.405
Liu and Cheng [32]	Circular	Bishop (1955)	Not required	Not available	1.405
Present study	General	Spencer [39]	Sequential quadratic programming (SQP)	Sequential quadratic programming (SQP)	1.350

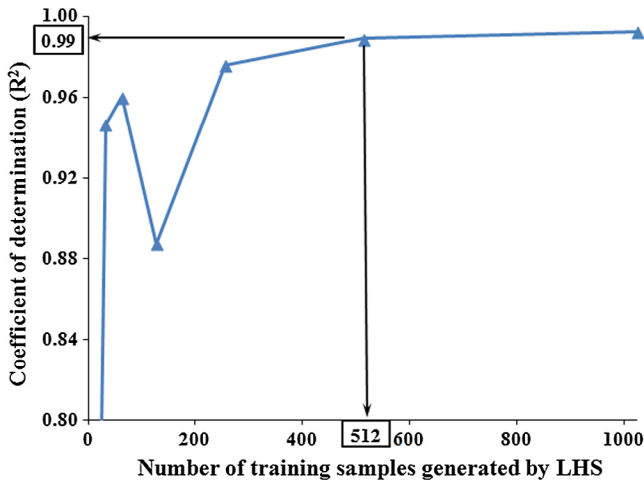


**Fig. 16.** Relationship between sample size and coefficient of determination ( $R^2$ ) (example 2).

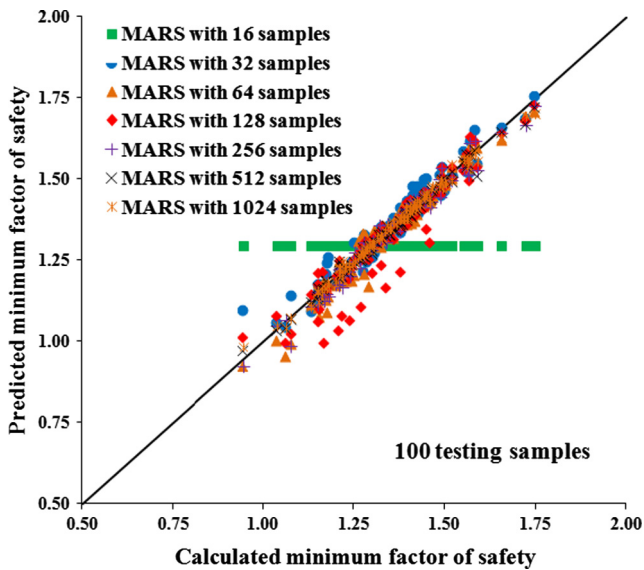


**Fig. 17.** Comparison between the values of  $FS_{min}$  predicted by different MARS models and those calculated by the Spencer method coupled with the SQP method in example 2.

Following the same procedure as in example 1, MARS models are also constructed to predict the locations of the critical slip surface with numbers of slices equals to 12. For 10 arbitrary set of samples, predicted locations of critical slip surfaces are compared with the calculated locations using the Spencer method coupled

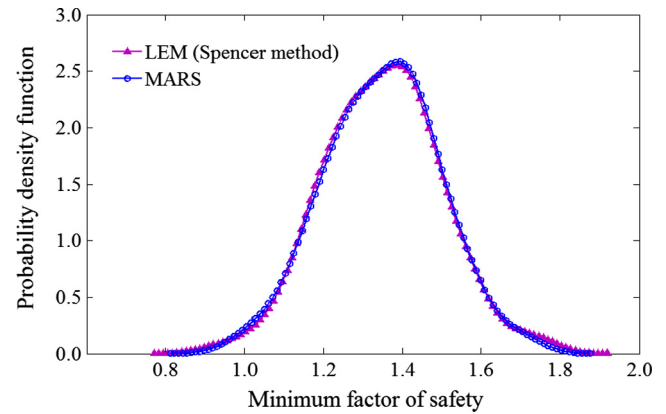


**Fig. 18.** Probability density function for minimum factor of safety based on the LEM based on Spencer method as well as the constructed MARS model in example 2.

with the SQP method in Fig. 19, which again indicates very good predictive capability of MARS model.

A MARS based sensitivity analysis by comparing the COV of the minimum factor of safety due the randomness added to slope system due to presence of specific random soil parameter is shown in Fig. 20(a). It is observed that  $\phi_3$  has the most significant influence to the system failure probability, followed by  $c_3$ . Another sensitivity study based on the MARS based surrogate model by comparing the variation of the minimum factor of safety with variation of the random strength parameters in a normalised scale is depicted in Fig. 20(b), which corroborates the observation made from Fig. 20 (a).

Like example 1, as the value of probability of failure obtained from the MCS is known to be sensitive to the number of simulations, trial simulations have been conducted using the constructed MARS-based RSM by varying the sample size from 2500 to 50,000. Fig. 21 shows the sensitivity of the probability of failure to the sample size when the seed number is taken as 28,061,987 (an arbitrary value). It is seen that beyond a sample size of 40,000 the probability of failure  $p_F$  is not sensitive to the sample size, and hence, the same has been adopted as the optimum number of simulations. The corresponding value of system failure probability is obtained as  $1.80 \times 10^{-2}$ . In Fig. 15, the 40,000 potential slip surfaces predicted MARS are plotted corresponding to the system probability of failure determined above. Figs. 22a and 22b present the histogram with the corresponding normal fit for the abscissas and ordinates of vertices 1, 4, 7, 10 and 13 respectively.

Table 4 presents a comparison of the failure probabilities obtained in the present analysis and that reported by previous investigators using different methodologies. It is observed that the value of the system failure probability ( $p_{F,s}$ ) obtained in the present analysis is higher than those reported in the previous studies using circular slip surfaces. It may therefore be concluded that

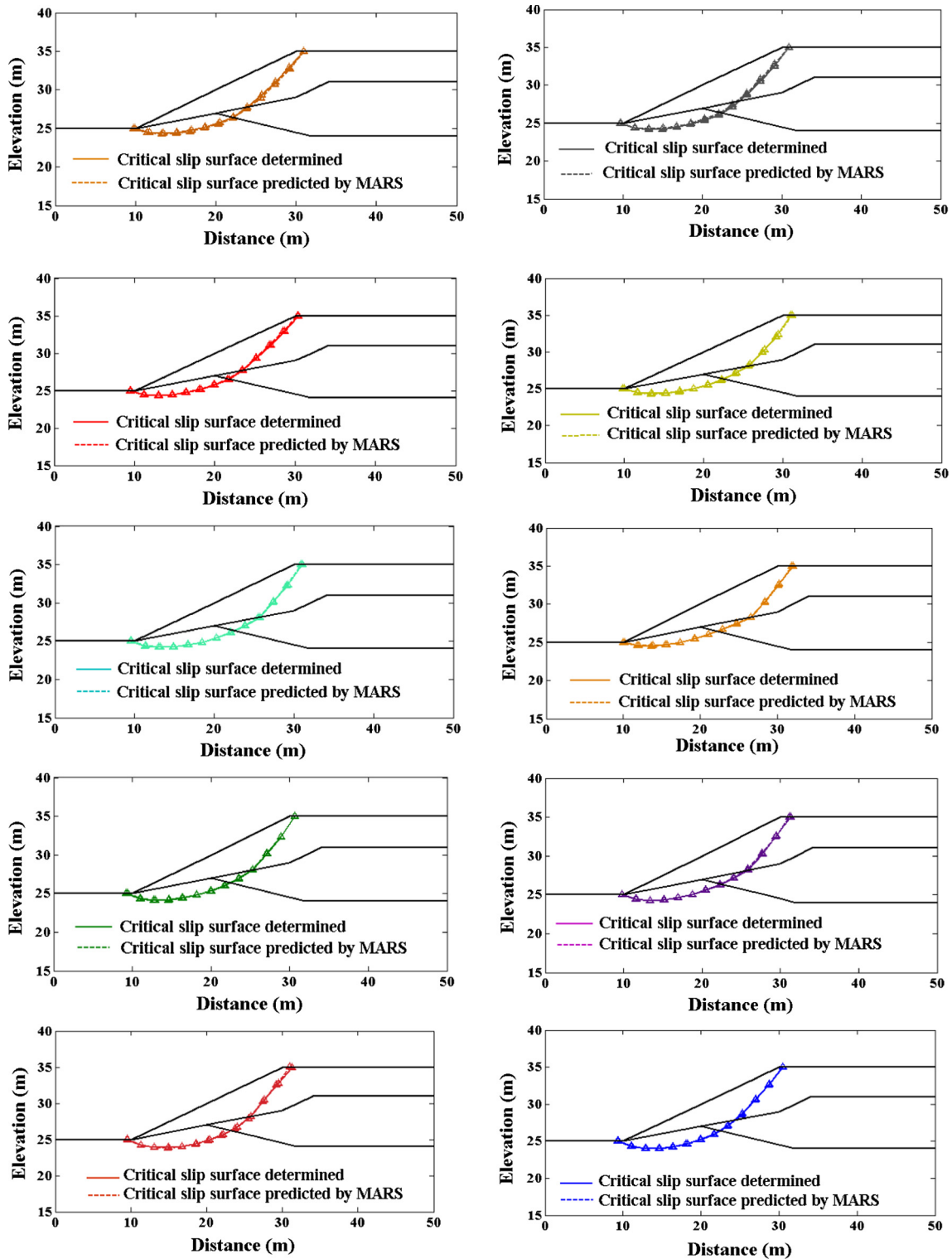


Fig. 19. Comparison between the locations of the critical slip surfaces determined by the Spencer method coupled with the SQP method and those predicted by MARS for 10 arbitrary set of samples in example 2.

system reliability analysis assuming the shape of the slip surfaces as circular underestimates the system failure probability. It is also noted that system failure probability value is higher than the value of probability of failure associated with the probabilistic critical slip surface (assuming single mode of failure), which is as per expectation.

### 3.5. Effect of noise

Like example 1, Fig. 23 shows some representative results describing the effect of noise on the minimum factor of safety. Similarly, Gaussian white noise with a specific value of variance ( $p$ ) in the range of 0.01–0.5 is introduced in the set of minimum factor of

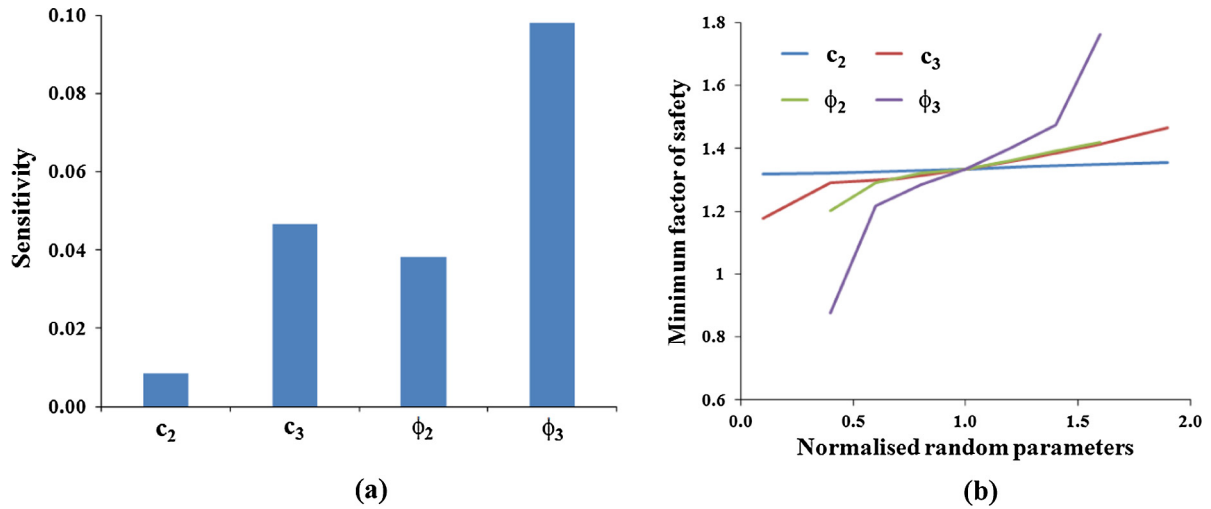


Fig. 20. Sensitivity studies based on the MARS model in example 2.

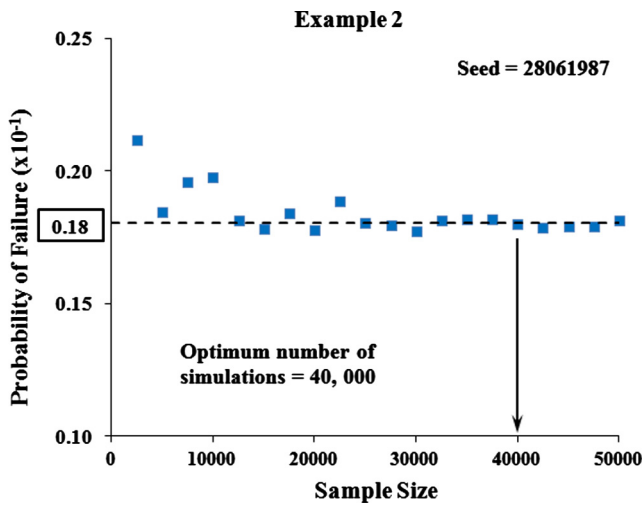


Fig. 21. Relationship between sample size and probability of failure (example 2).

safety, which is used for MARS model formation and the results provided in this article are obtained by using 500 such noisy datasets. The results presented for different values of variance are again compared with the probability density function of noise-free case to provide a comprehensive idea about the performance of MARS in uncertainty quantification under the influence of simulated noise for minimum factor of safety of earth slopes.

#### 4. Conclusions

Development of a surrogate based algorithm for system reliability analysis of earth slopes considering general slip surfaces in a Monte Carlo simulation framework is considered. The geomechanical parameters of the slope system have been treated as random variables. A multivariate adaptive regression splines (MARS) based approach is proposed under the framework of limit equilibrium method of slices to map the variation of minimum factor of safety caused due to uncertain input parameters. Similar procedure has also been used to predict the locations of critical slip surfaces. Spencer method valid for general slip surfaces [39] satisfying all

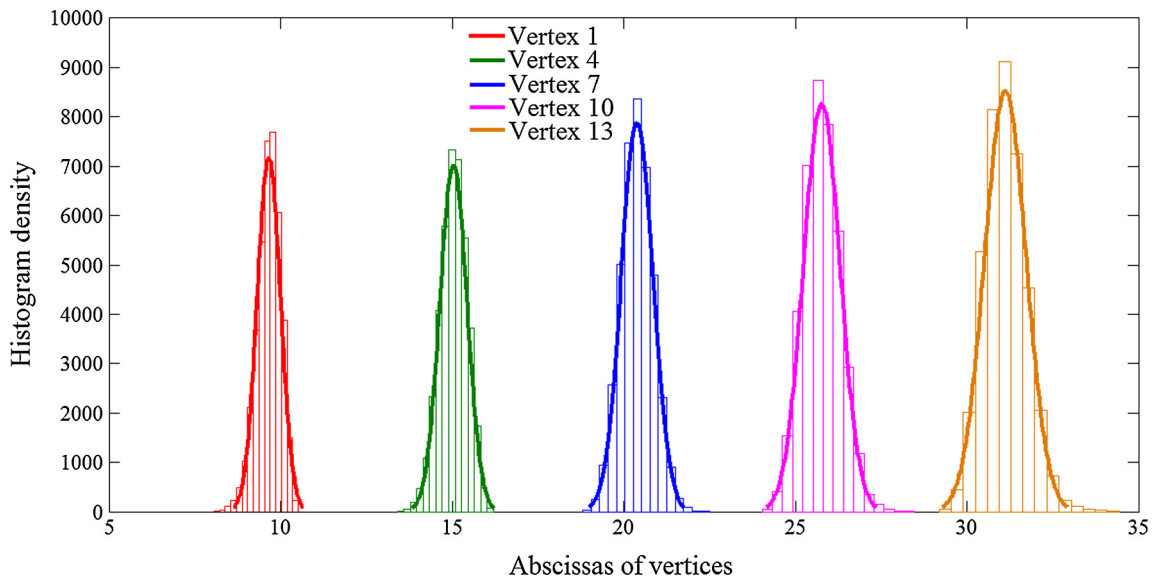


Fig. 22a. Histogram density plot of the abscissa of vertices in example 2.

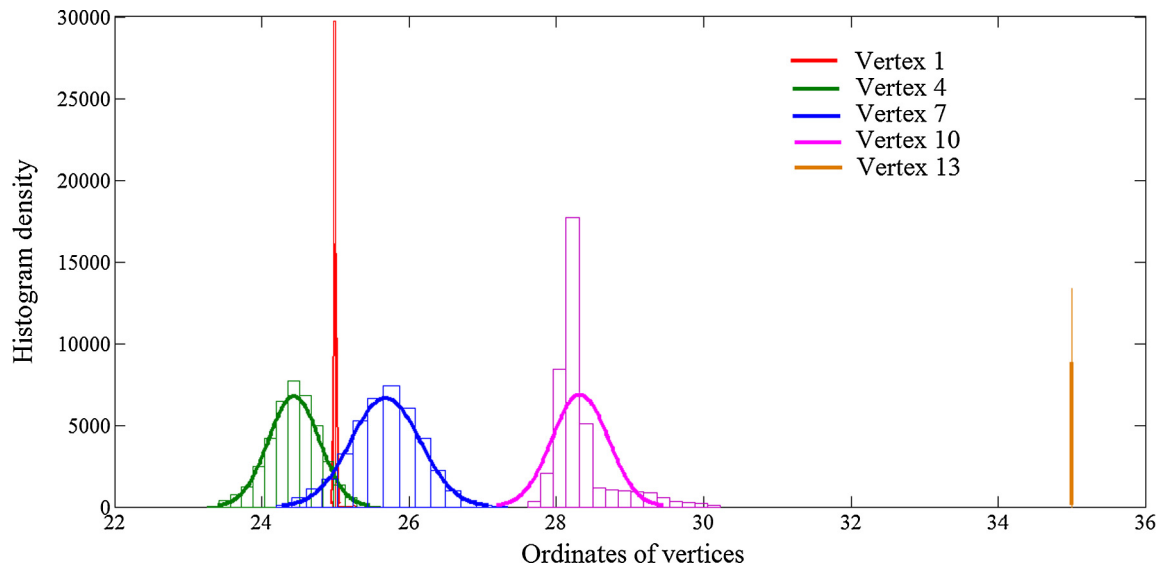


Fig. 22b. Histogram density plot of the ordinates of vertices in example 2.

**Table 4**  
Summary of results of probabilistic analyses for example 2.

Studies	Probabilistic method	Probability of failure, $p_F$ (%)
Ji and Low [14]	System reliability bounds based on the FORM	1.08–1.30%
	System reliability bounds based on the SORM	1.35–1.53%
Zhang et al. [16]	System failure probability based on MCS using the stratified RSM (50,000 samples)	1.34%
	Failure probability of the most critical slip surface based on MCS (50,000 samples)	1.01% (COV = 4.4%)
	System failure probability based on MCS (50,000 samples)	1.33% (COV = 3.8%)
Kang et al. [57]	System failure probability calculated based on the to the representative slip surfaces with MCS (50,000 samples)	1.08% (COV = 4.3%)
	System failure probability based on MCS using the GPR based RSM (10,00,000 samples)	1.59% (COV = 0.8%)
Liu and Cheng [32]	System failure probability based on MCS using the MARS based RSM (1,00,000 samples)	1.28% (COV = 2.78%)
	System failure probability based on MCS using the quadratic response surface method (QRSM) (1,00,000 samples)	1.55% (COV = 2.52%)
Present study	Failure probability of the most critical slip surface based on the FORM	1.25%
	System failure probability based on MCS using the MARS based RSM (40,000 samples)	1.80% (COV = 3.69%)

conditions of static equilibrium is used as a slope stability model in combination with the sequential quadratic programming (SQP) as a nonlinear programming technique of optimization. In order to compare the results of the reliability analysis, considering the single mode of failure, the FORM based probabilistic critical slip surface has also been located and the associated minimum reliability index (and the corresponding maximum probability failure) is determined. The effectiveness of the proposed procedure for system reliability analysis has been demonstrated by two benchmark example problems comprising an embankment underlain by a soft clay foundation and a complex slope in a multilayer ( $c$ ,  $\phi$ ) soil with arbitrary layer boundaries. Subsequently, the performance of MARS based uncertainty propagation algorithm under the effect of simulated noise is also investigated. For each of the two examples studied in this paper, once the MARS model is constructed and verified, the computational time needed for calculating the system failure probability based on the Monte Carlo simulation coupled with the MARS based surrogate is found to be negligible. Therefore, total computational expense is reduced by  $(128/30,000 \approx 1/234)$  times for the Example 1 and  $(512/40,000 \approx 1/78)$  times for the Example 2 with respect to the direct Monte Carlo simulation without compromising the accuracy of results. Thus, the proposed approach is an efficient tool for system reliability analysis.

Novelty of the present study includes the application of data driven MARS model to approximate the relationship of the mini-

um factor of safety functional and the location of the critical slip surface with the variation of the uncertain soil strength parameters. No assumptions are made on the shape of the slip surface (i.e. general slip surface is considered for the analyses), which is the first ever attempt in conjunction with any surrogate model to the best of authors' knowledge. A novel paradigm is proposed to account for the effect of simulated noise that can be implemented to other surrogate based analyses in the field of slope stability. Some of the key observations include:

1. The numerical results show that the system reliability analysis with circular slip surfaces can significantly underestimate the system failure probability of the soil slope.
2. The value of the system failure probability is higher than the value of the probability of failure associated with the probabilistic critical slip surface (assuming a single mode of failure), which is as per expectation.
3. The accuracy of the proposed approach is critically dependent on the number of training samples and the number of simulations. In-depth analyses are presented for determination of the optimum number of training samples as well as the optimum number of simulations with a reasonable accuracy.

Future works could include the proposed MARS based system reliability analysis algorithm to be implemented within probabilistic finite element analysis of slopes.

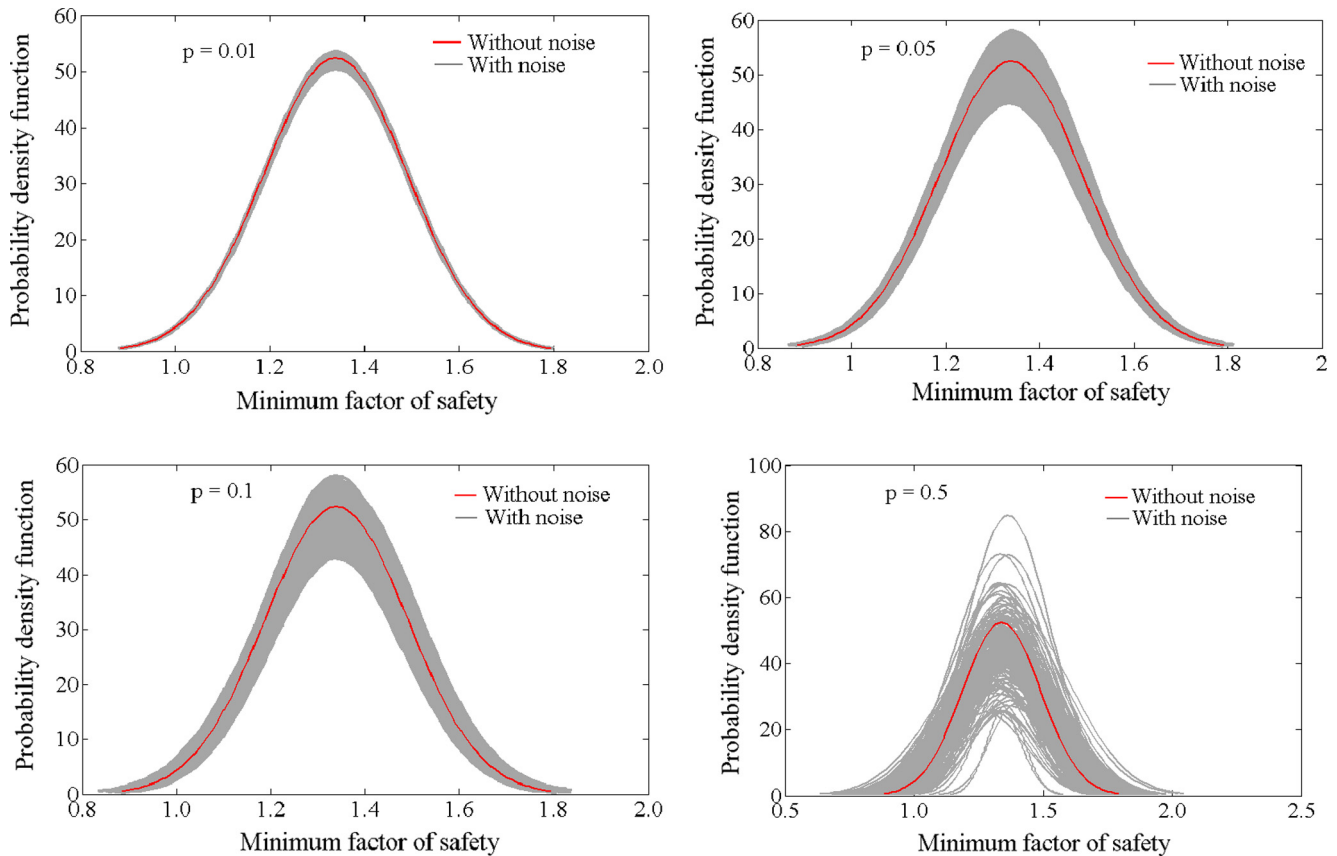


Fig. 23. Effect of noise on MARS based uncertainty quantification for minimum factor of safety of example 2.

## Acknowledgment

This research has been supported by the Newton-Bhabha PhD Placement Grant 2015–16 jointly funded by the British Council (United Kingdom) and the Department of Science and Technology (DST), Govt. of India for a collaborative research project at the Zienkiewicz Centre for Computational Engineering (ZCCE), Swansea University, UK. This support is gratefully acknowledged. TM acknowledges the financial support from the Swansea University through the award of Zienkiewicz Scholarship during the period of this work. SA acknowledges the financial support from the Royal Society of London through the Wolfson Research Merit award.

## References

- [1] Li KS, Lumb P. Probabilistic design of slopes. *Can Geotech J* 1987;24:520–35.
- [2] Hassan AH, Wolff TF. Search algorithm for minimum reliability index of earth slopes. *J Geotech Geoenviron Eng, ASCE* 1999;125(4):301–8.
- [3] Bhattacharya G, Jana D, Ojha S, Chakraborty S. Direct search for minimum reliability index of earth slopes. *Comput Geotech* 2003;30(6):455–62.
- [4] Metya S, Bhattacharya G. Probabilistic critical slip surface for earth slopes based on the first order reliability method. *Indian Geotech J* 2014;44(3):329–40.
- [5] Metya S, Bhattacharya G, Chowdhury R. Reliability analysis of slopes in strain-softening soils considering critical slip surfaces. *Innovative Infrastruct Solut* 2016;1:35. <http://dx.doi.org/10.1007/s41062-016-0033-8>.
- [6] Li DQ, Tang XS, Phoon KK. Bootstrap method for characterizing the effect of uncertainty in shear strength parameters on slope reliability. *Reliab Eng Syst Saf* 2015;140:99–106.
- [7] Cornell CA. Bounds on the reliability of structural systems. *J Struct Div* 1967;93(1):171–200.
- [8] Oka Y, Wu TH. System reliability of slope stability. *J Geotech Eng* 1990;116(8):1185–9.
- [9] Chowdhury RN, Xu DW. Geotechnical system reliability of slopes. *Rel Eng Syst Saf* 1995;47(3):141–51.
- [10] Ching J, Phoon KK, Hu YG. Efficient evaluation of reliability for slopes with circular slip surfaces using importance sampling. *J Geotech Geoenviron Eng* 2009;135(6):768–77.
- [11] Huang JS, Griffiths DV, Fenton GA. System reliability of slopes by RFEM. *Soils Found* 2010;50(3):343–53.
- [12] Wang Y, Cao Z, Au SK. Practical reliability analysis of slope stability by advanced Monte Carlo simulations in a spreadsheet. *Can Geotech J* 2011;48(1):162–72.
- [13] Zhang J, Zhang LM, Tang WH. New methods for system reliability analysis of soil slopes. *Can Geotech J* 2011;48(7):1138–48.
- [14] Ji J, Low BK. Stratified response surface for system probabilistic evaluation of slopes. *J Geotech Geoenviron Eng* 2012;138(11):1398–406.
- [15] Cho SE. First-order reliability analysis of slope considering multiple failure modes. *Eng Geol* 2013;154:98–105.
- [16] Zhang J, Huang HW, Juang CH, Li DQ. Extension of Hassan and Wolff method for system reliability analysis of soil slopes. *Eng Geol* 2013;160:81–8.
- [17] Li L, Wang Y, Cao Z. Probabilistic slope stability analysis by risk aggregation. *Eng Geol* 2014;176:57–65.
- [18] Low BK, Zhang J, Tang WH. Efficient system reliability analysis illustrated for a retaining wall and a soil slope. *Comput Geotech* 2011;38(2):196–204.
- [19] Ditlevsen O. Narrow reliability bounds for structural systems. *J Struct Mech* 1979;7(4):453–72.
- [20] Jiang SH, Huang JS. Efficient slope reliability analysis at low-probability levels in spatially variable soils. *Comput Geotech* 2016;75:18–27.
- [21] Li L, Wang Y, Cao Z, Chu X. Risk de-aggregation and system reliability analysis of slope stability using representative slip surfaces. *Comput Geotech* 2013;53:95–105.
- [22] Jiang SH, Li DQ, Cao ZJ, Zhou CB, Phoon KK. Efficient system reliability analysis of slope stability in spatially variable soils using Monte Carlo simulation. *J Geotech Geoenviron Eng (ASCE)* 2015;141(2):04014096.
- [23] Li L, Chu XS. Multiple response surfaces for slope reliability analysis. *Int J Numer Anal Methods Geomech* 2015;39(2):175–92.
- [24] Zhang J, Huang HW, Phoon KK. Application of the Kriging-based response surface method to the system reliability of soil slopes. *J Geotech Geoenviron Eng (ASCE)* 2013;139(4):651–5.
- [25] Yi P, Wei K, Kong X, Zhu Z. Cumulative PSO-Kriging model for slope reliability analysis. *Probab Eng Mech* 2015;39:39–45.
- [26] Cho SE. Probabilistic stability analyses of slopes using the ANN-based response surface. *Comput Geotech* 2009;36(5):787–97.
- [27] Kang F, Li J. Artificial bee colony algorithm optimized support vector regression for system reliability analysis of slopes. *J Comput Civ Eng* 2015;04015040.



- [28] Chowdhury R, Rao BN. Probabilistic stability assessment of slopes using high dimensional model representation. *Comput Geotech* 2010;37(7–8):876–84.
- [29] Li DQ, Zheng D, Cao ZJ, Tang XS, Phoon KK. Response surface methods for slope reliability analysis: review and comparison. *Eng Geol* 2016;203:3–14.
- [30] Hassan AH, Wolff TF. Closure to ‘Search Algorithm for Minimum Reliability Index of Earth Slopes’ by Hassan AH and Wolff TF. *J Geotechn Geoenviron Eng, ASCE* 2001;127(02):198–200.
- [31] Hong H, Roh G. Reliability evaluation of earth slopes. *J Geotech Geoenviron Eng* 2008;134(12):1700–5.
- [32] Liu LL, Cheng YM. Efficient system reliability analysis of soil slopes using multivariate adaptive regression splines-based Monte Carlo simulation. *Comput Geotech* 2016;79:41–54.
- [33] Friedman JH. Multivariate adaptive regression splines. *Ann Stat* 1991;19(1):1–67.
- [34] Sudjianto A, Juneja L, Agrawal A, Vora M. Computer aided reliability and robustness assessment. *Int J Reliab, Qual Saf* 1998;5:181–93.
- [35] Samui P. Multivariate adaptive regression spline (MARS) for prediction of elastic modulus of jointed rock mass. *Geotech Geol Eng* 2013;31(1):249–53.
- [36] Dey S, Mukhopadhyay T, Naskar S, Dey TK, Chalak HD, Adhikari S. Probabilistic characterization for dynamics and stability of laminated soft core sandwich plates. *J Sandwich Struct Mater*. SAGE Publication; 2016. In press.
- [37] Mukhopadhyay T. A multivariate adaptive regression splines based damage identification methodology for web core composite bridges including the effect of noise. *J Sandwich Struct Mater*. SAGE Publication; 2016. In Press.
- [38] Chowdhury R, Flentje P, Bhattacharya G. Geotechnical slope analysis. Balkema: CRC Press; 2010. p. 737.
- [39] Spencer E. The thrust line criterion in embankment stability analysis. *Geotechnique* 1973;23(1):85–100.
- [40] Duncan JM, Wright SG. The accuracy of equilibrium methods of slope stability analysis. *Eng Geol* 1980;16(1–2):5–17.
- [41] Bhattacharya G, Basudhar PK. A new procedure for finding critical slip surfaces in slope stability analysis. *Indian Geotech J* 2001;31(1):149–72.
- [42] Rao SS. Engineering optimization: theory and practice. 4th ed. New York: Wiley; 2009.
- [43] Haldar A, Mahadevan S. Probability reliability and statistical methods in engineering design. John Wiley and Sons; 2000.
- [44] Metya S, Bhattacharya G. Probabilistic stability analysis of the Bois Brule levee considering the effect of spatial variability of soil properties based on a new discretization model. *Indian Geotech J* 2016;46(2):152–63.
- [45] Metya S, Bhattacharya G. Reliability analysis of earth slopes considering spatial variability. *Geotech Geol Eng – An Int J* 2016;34(1):103–23.
- [46] Craven P, Wahba G. Smoothing noisy data with spline functions. *Numer Math* 1979;31:377–403.
- [47] Crino S, Brown DE. Global optimization with multivariate adaptive regression splines. *IEEE Trans Syst Man Cybern Part B: Cybern* 2007;37(2).
- [48] Bourdeau PL, Amundaray JI. Non-parametric simulation of geotechnical variability. *Géotechnique* 2005;55(2):95–108.
- [49] Ang AHS, Tang WH. Probability concepts in engineering: emphasis on applications to civil and environmental engineering. 2nd ed. New York: John Wiley & Sons Inc; 2007.
- [50] Christian JT, Ladd CC, Baecher GB. Reliability applied to slope stability analysis. *J Geotech Geoenviron Eng, ASCE* 1994;120(12):2180–207.
- [51] Mukhopadhyay T, Naskar S, Dey S, Adhikari S. On quantifying the effect of noise in surrogate based stochastic free vibration analysis of laminated composite shallow shells. *Compos Struct* 2016;140:798–805.
- [52] Nejad FB, Rahai A, Esfandiari A. A structural damage detection method using static noisy data. *Eng Struct* 2005;27:1784–93.
- [53] Mukhopadhyay T, Chowdhury R, Chakrabarti A. Structural damage identification: a random sampling-high dimensional model representation approach. *Adv Struct Eng* 2016;19(6):908–27.
- [54] Ji J, Liao HJ, Low BK. Modeling 2-D spatial variation in slope reliability analysis using interpolated autocorrelations. *Comput Geotech* 2012;40:135–46.
- [55] US Army Corps of Engineers. Introduction to probability and reliability methods for use in geotechnical engineering, in ETL 1110-2-547; 1995.
- [56] Donald IB, Giam PSK. Soil slope stability programs review, ACADS – Association for Computer Aided Design, Melbourne, Australia, Report U255; 1989.
- [57] Kang F, Han S, Salgado R, Li J. System probabilistic stability analysis of soil slopes using Gaussian process regression with Latin hypercube sampling. *Comput Geotech* 2015;63:13–25.